

FINAL REPORT

Grant # DE-FG02-03ER15461

Project Title: Principles of water oxidation and O₂-based hydrocarbon transformation by multinuclear catalytic sites

Application Institution: Emory University
1599 Clifton Rd., NE 4th Floor
Mail Stop: 1599-001-1BA, Atlanta, GA. 30322

PI / PD: Djamaladdin Musaev, Ph.D.
Cherry L. Emerson Center for Scientific Computation, Room 518
Emory University
1515 Dickey Dr. NE
Atlanta, GA 30322
Tel. 404-727-2382; Fax: 404-727-7412
e-mail: dmusaev@emory.edu

Co-PI: Craig L. Hill, Ph.D.
Department of Chemistry
Emory University
1515 Dickey Dr. NE
Atlanta, GA 30322, Tel. 404-727-6611
e-mail: chill@emory.edu

Co-PI: Keiji Morokuma, Ph.D.
Cherry L. Emerson Center for Scientific Computation
Emory University
1515 Dickey Dr. NE
Atlanta, GA 30322, Tel: 404-727-2380
morokuma@emory.edu

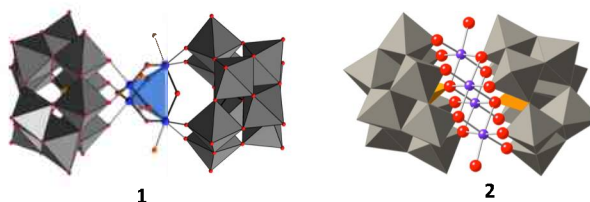
DOE Office of Science Program Manager Contact
Raul Miranda
Program Manager
Catalysis and Chemical Transformations
Chemical Sciences, Geosciences and Biosciences Division
Office of Basic Energy Sciences
SC-14 / Germantown Building
U.S. Department of Energy
1000 Independence Ave., S.W.
Washington, DC 20585-1290
Tel. 301-903-8014

Summary/Abstract

The central thrust of this integrated experimental and computational research program was to obtain an atomistic-level understanding of the structural and dynamic factors underlying the design of catalysts for water oxidation and selective reductant-free O₂-based transformations. The focus was on oxidatively robust polyoxometalate (POM) complexes in which a catalytic active site interacts with proximal metal centers in a synergistic manner. Thirty five publications in high-impact journals arose from this grant.

I. Developing an oxidatively and hydrolytically stable and fast water oxidation catalyst (WOC), a central need in the production of green fuels using water as a reductant, has proven particularly challenging. During this grant period we have designed and investigated several carbon-free, molecular (homogenous), oxidatively and hydrolytically stable WOCs, including the Rb₈K₂[{Ru₄O₄(OH)₂(H₂O)₄}(γ-SiW₁₀O₃₆)₂]-25H₂O (**1**) and [Co₄(H₂O)₂(α-PW₉O₃₄)₂]¹⁰⁻ (**2**) (Figure 1). Although complex **1** is fast, oxidatively and hydrolytically stable WOC, Ru is neither abundant nor inexpensive. Therefore, development of a stable and fast carbon-free homogenous WOC, based on earth-abundant elements became our highest priority. In 2010, we reported the first such catalyst, complex **2**. This complex is substantially faster than **1** and stable under homogeneous conditions. Recently, we have extended our efforts and reported a V₂-analog of the complex **2**, i.e. [Co₄(H₂O)₂(α-VW₉O₃₄)₂]¹⁰⁻ (**3**), which shows an even greater stability and reactivity.

Figure 1. X-ray structures of the WOCs **1** and **2**. Counter cations and Hydrogen atoms are omitted for clarity. In **1**, highlighting the central [Ru₄(μ-O)₄(μ-OH)₂(H₂O)₄]⁶⁺ core (Ru in blue, μ-O in red, and O(H₂) in orange). In **2**, in the Co₄O₁₆ core: Co in purple, O/OH₂(terminal) in red; PO₄ in orange tetrahedra. The polytungstate fragments are shown as gray polyhedra.

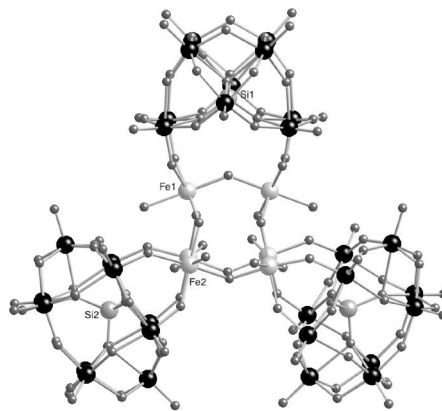


We succeeded in: (a) immobilizing catalysts **1** and **2** on the surface of various electrodes, and (b) elucidating the mechanism of O₂ formation and release from complex **1**, as well as the Mn₄O₄L₆ “cubane” cluster. We have shown that the direct O-O bond formation is the most likely pathway for O₂ formation during water oxidation catalyzed by **1**.

II. Oxo transfer catalysts that contain two proximal and synergistically interacting redox active metal centers in the active site form another part of considerable interest of our grant because species with such sites [including methane monooxygenase (MMO) and more] are some of the most effective oxygenase catalysts known. Our team conducted the following research on γ-M₂-Keggin complexes: (a) investigated stability of the trimer [{Fe₃(OH)₃(H₂O)₂}₃(γ-SiW₁₀O₃₆)₃]¹⁵⁻, **4**, in water, and developed the chemistry and catalysis of the di-iron centered POM, [γ(1,2)-SiW₁₀{Fe(OH)₂O₃₈}]⁶⁻, **5**, in organic solvents (Figure 2). We also study the thermodynamic and structural stability of γ-M₂-Keggin in aqueous media for different M's (d-electron metals).

We have defined two structural classes of POMs with proximally bound d-electron metal centers. We refer to these structural isomers of the $\{\gamma\text{-M}_2\text{SiW}_{10}\}$ family of POMs as “in-pocket” and “out-of pocket”. We have elucidated the factors controlling the structure and stability of the V, Fe, Ru, Tc, Mo and Rh derivatives of $[(\text{SiO}_4)\text{M}_2(\text{OH})_2\text{W}_{10}\text{O}_{32}]^{4-}$ using a

Figure 2. X-ray structure of the $[\{\text{Fe}_2(\text{OH})_3(\text{H}_2\text{O})_2\}_3(\gamma\text{-SiW}_{10}\text{O}_{36})_3]^{15-}$, **4**, polyanion (crystallized as the $\text{K}_7[(\text{CH}_3)_2(\text{NH}_2)]_8$ salt from H_2O).



range of computational tools. We have: (a) demonstrated that heteroatom X in these polyanions may function as an “internal switch” for defining the ground electronic states and, consequently, the reactivity of the $\gamma\text{-M}_2\text{-Keggin}$ POM complexes; (b) elucidated reactivity of divacant lacunary species and polyperoxotungstates (PPTs), $\{\text{X}^{n+}\text{O}_4[\text{WO}(\text{O}_2)_2]_4\}^{n-}$, which could be degradation products of $\gamma\text{-M}_2\text{-Keggin}$ complexes in aqueous media; (c) elucidated the role of the POM ligand in stabilization of $\{\text{Ru}_2\}$ and $\{(\text{Ru-oxo})_2\}$ fragments in the reactant and product of the reaction of $\{\gamma\text{-}[(\text{X}^{n+}\text{O}_4)\text{Ru}_2(\text{OH})_2\text{W}_{10}\text{O}_{32}]\}^{(8-n)-}$ (where $\text{X} = \text{Si}^{4+}$, P^{5+} and S^{6+}) with O_2 , and (d) the mechanisms of olefin epoxidation catalyzed by these di-d-transition metal substituted and divacant lacunary $\gamma\text{-M}_2\text{-Keggin}$ complexes.

III. Complementing the efforts presented above was the development of less time-consuming but reasonably accurate computational methods allowing one to explore more deeply large catalytic systems. We developed Reactive Force Field (ReaxFF) to study interaction of the targeted POMs with water, proton and hydroxide ions in the liquid phase. We tested our ReaxFF parameters on the Lindqvist POMs, $\text{M}_6\text{O}_{19}^{n-}$, where $\text{M} = \text{Nb}$ and Ta . These parameters are made available as part of the ReaxFF code.

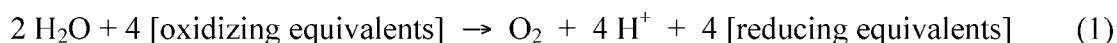
In addition, we have developed parameters for Sc, Ti, Fe, Co and Ni in combination with H, C, N, O, as well as the same metal (M-M) for the spin-polarized self-consistent-charge density-functional tight-binding (DFTB) method. Test calculations showed that the DFTB method with the present parameters in most cases reproduces structural properties very well. These parameters are made available as part of the DFTB code.

Thus, this DOE BES funded research project has clarified several key areas impacting (a) water oxidation and O_2 -based hydrocarbon transformation, (b) stabilization of key structures and catalytic intermediates in such processes, (c) immobilization of molecular catalysts on metal oxide surfaces, and (d) application of optimal computational methods to study reaction dynamics in large systems.

Major achievements:

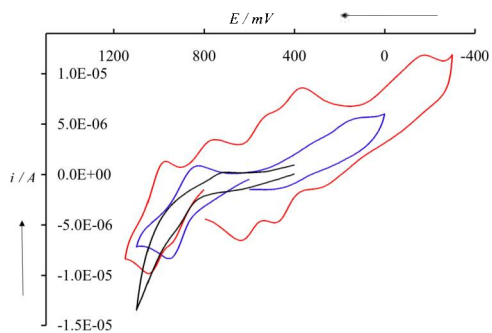
I. Molecular, carbon-free, stable and fast catalysts for water oxidation.

I.a. Our team has designed the first homogeneous (molecular) catalyst for H₂O oxidation that is free of oxidatively unstable organic structure of any kind. This complex, Rb₈K₂[{Ru₄O₄(OH)₂(H₂O)₄}(γ-SiW₁₀O₃₆)₂] \cdot 25H₂O (**1**), contains four Ru centers that have reduction potentials in the exact range needed to oxidize H₂O. We first demonstrated that **1** (see Figure 1) can be reversibly oxidized and reduced by four electrons (cyclic voltammograms in Figure 3), a critical prerequisite for the oxidation of H₂O, i.e. eq 1, and then we have shown that **1** catalyzed eq 1 using strong oxidants (e.g. “oxidizing equivalents” in eq 1 = [Ru(bpy)₃]³⁺, etc.)



Achieving a stable molecular catalyst for H₂O oxidation to O₂ would constitute a major step forward. Solid state catalysts (i.e. surfaces) are known that are stable to the rigors of sustained H₂O oxidation, but until publication of our paper in 2008 there have been no stable molecular catalysts for such processes. The reason for this is that organic ligands are thermodynamically unstable to oxidative degradation, ultimately to H₂O and CO₂. Molecular catalysts are intensely sought because these could be interfaced with almost any type of photosensitizer system – Grätzel cell components, soluble H₂ evolution species, modified biological (e.g. chloroplast) formulations and solid state devices. This isn't true for heterogeneous (i.e. insoluble and solid state) catalysts.

Figure 3. CVs of 1 mM **1** in 0.1 M HCl (pH 1.0, red curve), in 0.4 M sodium acetate buffer (pH 4.7, blue curve), and of 0.6 mM **1** (pH 7.0, black curve). Scans start at the rest potentials, 800, 600 and 400 mV, respectively and potentials are relative to a Ag/AgCl (3 M NaCl) reference electrode.



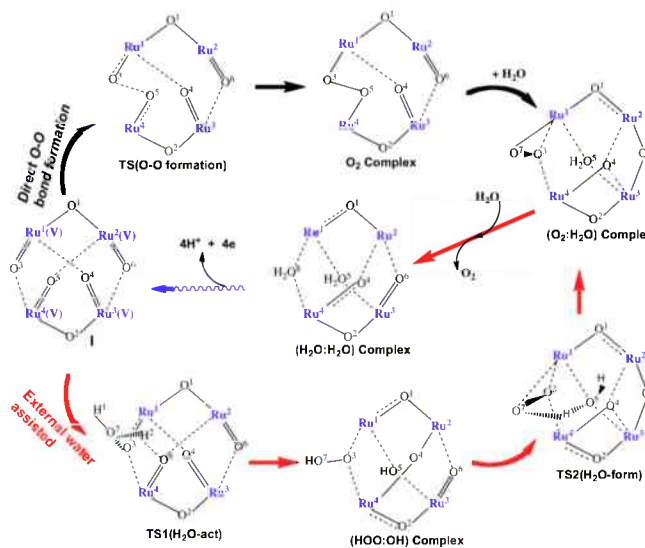
We have studied the geometries and electronic structures of the catalyst **1** in five different oxidation states: [$\{\text{Ru}_4\text{O}_4(\text{OH})_2(\text{H}_2\text{O})_4\}(\gamma\text{-SiW}_{10}\text{O}_{36})_2$]¹⁰⁻, **1(0)**, [$\{\text{Ru}_4\text{O}_4(\text{OH})_2(\text{H}_2\text{O})_4\}(\gamma\text{-SiW}_{10}\text{O}_{36})_2$]⁹⁻, **1(+1)**, [$\{\text{Ru}_4\text{O}_4(\text{OH})_2(\text{H}_2\text{O})_4\}(\gamma\text{-SiW}_{10}\text{O}_{36})_2$]⁸⁻, **1(+2)**, [$\{\text{Ru}_4\text{O}_4(\text{OH})_2(\text{H}_2\text{O})_4\}(\gamma\text{-SiW}_{10}\text{O}_{36})_2$]⁷⁻, **1(+3)**, and [$\{\text{Ru}_4\text{O}_4(\text{OH})_2(\text{H}_2\text{O})_4\}(\gamma\text{-SiW}_{10}\text{O}_{36})_2$]⁶⁻, **1(+4)**, using the density functional theory. It was found that the several HOMOs and LUMOs of these complexes are bonding and anti-bonding orbitals of the [$\text{Ru}_4\text{O}_4(\text{OH})_2(\text{H}_2\text{O})_4$]⁶⁺ core, and the first four one-electron oxidations of **1(0)**, leading to formation of **1(+1)**, **1(+2)**, **1(+3)** and **1(+4)**, respectively, involve only {Ru₄O₄} core orbitals. In other words, catalyst instability due to ligand oxidation in the widely studied “blue dimer”, [(bpy)₂(O)Ru^V-(μ-O)-Ru^V(O)(bpy)₂]⁴⁺, is not operable for **1**: the latter all-inorganic catalyst is predicted to be stable under water oxidation turnover conditions. The calculated HOMOs and LUMOs of **1** are very close in energy and exhibit a “quasi-continuum” or “nanoparticle-type”

electronic structure similar to that of nano-sized transition metal clusters. This conclusion closely correlates with the experimentally reported oxidation and reduction features of **1**.

We elucidated the mechanisms of water oxidation by **1**. For this purpose, initially we studied proton-coupled-electron-transfer processes by calculating the structures of $[\{\text{Ru}_4\text{O}_4(\text{OH})_2(\text{H}_2\text{O})_4\}(\gamma\text{-SiW}_{10}\text{O}_{36})_2]^{10-}$, **1**, $[\{\text{Ru}_4\text{O}_4(\text{OH})_3(\text{H}_2\text{O})_3\}(\gamma\text{-SiW}_{10}\text{O}_{36})_2]^{10-}$, **1(-H)**, $[\{\text{Ru}_4\text{O}_4(\text{OH})_4(\text{H}_2\text{O})_2\}(\gamma\text{-SiW}_{10}\text{O}_{36})_2]^{10-}$, **1(-2H)**, $[\{\text{Ru}_4\text{O}_4(\text{OH})_5(\text{H}_2\text{O})\}(\gamma\text{-SiW}_{10}\text{O}_{36})_2]^{10-}$, **1(-3H)**, and $[\{\text{Ru}_4\text{O}_4(\text{OH})_6\}(\gamma\text{-SiW}_{10}\text{O}_{36})_2]^{10-}$, **1(-4H)**.

Figure 4. The “direct O-O bond formation” and “external-water-assisted” mechanisms of O_2 -formation involving catalyst **1(+4)**.

It was shown that the chemical potential (vs. NHE) required for process involving four PCET events is 1.23 eV per PCET event, which is slightly higher than 1.21 eV calculated for the water oxidation (the experimentally reported value for water oxidation (at pH=0) is 1.23 eV). Thus, the **1** to **1(-4H)** four-electron oxidation process



is sufficient for water oxidation by **1(+4)**. We elucidated the “direct O-O bond formation” and “external-water-assisted” mechanisms of O_2 formation catalyzed by **1(+4)** (see Figure 4). It was found that the “direct O-O bond formation” mechanism proceeds via 16.9 kcal/mol rate determining barrier at the O-O formation transition state, while the “external-water-assisted” mechanism requires 24.8 kcal/mol energy barrier (associated with **TS1(H₂O-act)**). Thus, the direct O-O bond formation is the most likely pathway for O_2 formation during water oxidation catalyzed by **1**.

We succeeded in immobilizing catalyst **1** on carbon-based supports, including those used as electrode materials. The most stable electrode we have obtained thus far involves functionalized multiwall carbon nanotubes adsorbed on the surface of either glassy carbon or graphite electrodes. The modified graphite electrode was utilized in bulk water electrolysis with a Pt wire as a cathode. Under minimally optimized conditions high electron efficiency was achieved. Dihydrogen and dioxygen are formed in 2:1 ratio. However, an increase in the applied potential results in the unwanted oxidation of graphite. For that reason, we replaced graphite with an FTO (fluorine-doped tin oxide) electrode coated with a thin layer of TiO_2 . We synthesized a phosphonated viologen derivative and subsequently deposited it on this TiO_2 -FTO electrode. The presence of the phosphonated viologen derivative on the electrode rendered this surface positively charged and thus able to strongly and rapidly bind the negatively charged POMs.

The reaction of catalyst **1** with alcohols also was studied in an attempt to develop a catalyst for selective oxidation of alcohols by ambient air. This reaction results in two-electron reduction of **1(0)** and the stoichiometric formation of ketones (or aldehydes). Kinetically, the reaction proceeds in two steps: a moderately fast one-electron reduction of **1(0)** to **1(+1)** followed by a second very slow one-electron reduction of POM. The reaction product, the 2-electron-reduced complex, **1(+2)**, is not efficiently re-oxidized by O₂.

I.b. Multi-Co-oxo cluster systems: Co₄-based soluble, stable and fast WOCs. The Ru₄O₄-based catalyst **1** is fast, oxidatively and hydrolytically stable, but Ru is neither abundant nor inexpensive and thus very likely prohibitive for use on a realistic scale. Therefore, development of a stable and fast carbon-free homogenous WOC, based on earth-abundant elements would be of great interest. In 2010, we reported the first such catalyst. This complex, [Co₄(H₂O)₂(α-PW₉O₃₄)₂]¹⁰⁻, (**2**, called as **Co4P2**), has a Co₄O₁₆ core stabilized by oxidatively resistant polytungstate ligands (Figure 1). This catalyst is free of carbon-based ligands (thus oxidatively stable) and it self assembles in water from salts of earth abundant elements (Co, W and P). With [Ru(bpy)₃]³⁺ (bpy = 2,2'-bipyridine) as an oxidant, we observe catalytic turnover frequencies for O₂ production ≥ 5 s⁻¹ at pH 8.

Complex **2** is substantially faster water oxidation catalyst than **1**. The pH dependence of the rate of O₂ evolution by **2** reflects the pH dependence of the 4-electron H₂O/O₂ couple. Extensive spectroscopic, electrochemical, and inhibition studies firmly indicate that **2** is stable under catalytic turnover conditions: neither hydrated cobalt ions nor cobalt hydroxide/oxide particles form *in situ*. However, at pH 8 in phosphate buffer it forms a cobalt-oxide (CoO_x) film on the surface of glassy carbon electrode if a high positive potential is applied. We have shown that under homogeneous conditions the complex, **2**, itself, is the true catalyst and not the products of its decomposition.

Computational studies of the electronic structure of **2** provide additional support for the oxidative stability of the polytungstate ligands. The four top HOMO's of a high-spin ground state of **2** are mostly cobalt core orbitals, and there is almost no involvement of tungstate orbitals. These findings indicate that the polytungstate ligands are unlikely to participate in the water oxidation reaction and should be effectively inert under catalytic conditions.

Just recently, we have developed and are in the process of reporting a new molecular water oxidation catalyst, Na₁₀[Co₄(H₂O)₂(VW₉O₃₄)₂], (**3**, called as **Co4V2**), that is structurally analogous to **2** but appears to be more hydrolytically stable under basic conditions and shows much higher catalytic activity than **2** [see Hill, C. L.; Musaev, D. G. and coworkers, *J. Am. Chem. Soc.*, **2014**, *136*, 9268-9271].

During this grant period, we also have reported several other multi-Co catalysts such as **Co4Si2** and **Co9-POM**. However, all these systems have showed much lower catalytic activity compared to our **CoP2** and **Co4V2** catalysts.

I.c. Insights into the mechanism of O₂ formation and release from the Mn₄O₄L₆ “cubane” cluster. In order to probe photoinduced water oxidation catalyzed by the Mn₄O₄L₆ cubane clusters, we have computationally studied the mechanism and the controlling factors of O₂ formation from the [Mn₄O₄L₆]-containing catalyst, **6** (Figure 5).

It was demonstrated that photolytic dissociation of an $L^- = \text{H}_2\text{PO}_2^-$ ligand from **6** significantly shortens the O^1-O^1 distance in a Mn_4O_4 -core and facilitates formation of the O^1-O^1 bond. The O-O bond formation starts from the resulting cationic complex $[\text{Mn}_4\text{O}_4\text{L}_5]^+$, **I**, and proceeds with a 28.3 (33.4) kcal/mol rate-determining energy barrier at **TS1**. This step of the reaction is a 2-electron oxidation/reduction process, during which two oxo ligands are transformed into a $\mu^2:\eta^2-\text{O}_2^{2-}$ unit, and two (“distal”) Mn centers are reduced from the 4+ to the 3+ oxidation state. Next two-electron oxidation/reduction occurs by “dancing” of the O_2^{2-} fragment between the Mn^1 and $\text{Mn}^2/\text{Mn}^{2'}$ -centers but maintaining its strong coordination to the Mn^1 -center. Thus, as a result of this 4-electron oxidation-reduction process, the Mn-centers of the Mn_4 -core of **I** transform from $\{\text{Mn}^1(\text{III})-\text{Mn}^{1'}(\text{III})-\text{Mn}^2(\text{IV})-\text{Mn}^{2'}(\text{IV})\}$ to $\{\text{Mn}^1(\text{II})-\text{Mn}^{1'}(\text{II})-\text{Mn}^2(\text{III})-\text{Mn}^{2'}(\text{III})\}$ in **VI**. In other words, upon O_2 formation in cationic complex $[\text{Mn}_4\text{O}_4\text{L}_5]^+$, **I**, each Mn-center of **I** is reduced by one electron. The overall reaction $\text{I} \rightarrow \text{VI} + \text{O}_2$ is found to be exothermic by 15.4 (10.5) kcal/mol. We conducted careful analysis of the lowest spin states, as well as geometries of all reactants, intermediates, transition states and products of the overall reaction.

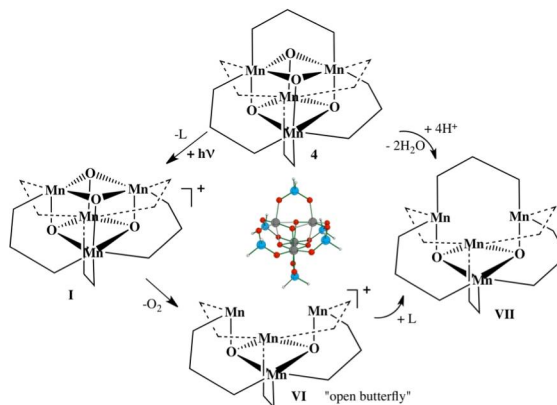


Figure 5. Schematic presentation of the mechanism of O_2 formation and release from $\text{Mn}_4\text{O}_4\text{L}_6$ “cubane” cluster.

II. POM systems with two adjacent d-electron transition metals as a catalyst for selective reductant-free O_2 -based transformations.

The development of catalysts for the selective (non-radical-chain), reductant-free O_2 -based oxidation of organic substrates remains one of the most sought goals in chemistry. Very few molecules or materials exhibit this ability; radical-chain processes (autoxidations) still dominate industrial and nearly all other reactions based on O_2 or air.

We began investigations on the di-iron centered POM, $[\gamma(1,2)\text{-SiW}_{10}\{\text{Fe}(\text{OH})\}_2\text{O}_{38}]^{6-}$, **5**, since it was one member of a possibly large family of synthetically accessible POM complexes containing two proximal redox-active d-metal centers in the active site, a feature seen in many other effective biological and synthetic catalysts, and not just the intensely investigated enzymes MMO and RNR. We have defined two structural classes of POMs, A and B in Figure 6. As seen from this figure, in structure A, the M centers are surrounded by POM oxygens, directly interact with the red internal oxygens, O_x , we refer to this structure as “in-pocket” (the Fe centers reside in a pocket of the multidentate POM ligand). In structure B, the $\text{Fe}-\text{O}_x$ bonds are broken and replaced by Fe bonds to terminal. As a result the Fe centers in Figure 6B move away from the body of the POM and hence the description “out-of-pocket”.

We successfully determined that a combination of K^+ and dimethyl ammonium cation facilitated crystallization of “5” from H_2O . This was a significant because H_2O is the optimally desirable solvent for many homogeneous catalytic oxidations. To our surprise, the structure of the $\gamma(1,2)$ - $SiW_{10}Fe_2$ POM was not the in-pocket 5 but rather a trimeric polyanion of formula

$$[\{Fe_3(OH)_3(H_2O)_2\}_3(\gamma-SiW_{10}O_{36})_3]^{15-} \quad (4)$$

constituted by three out-of-pocket $\gamma(1,2)$ - $SiW_{10}Fe_2$ units (Figure 2).

Importantly, however, we have established that the form of $\gamma(1,2)$ - $SiW_{10}Fe_2$ isolable from H_2O , namely the trimer

4, does catalyze selective O_2 -based oxidations of organic compounds. This complex is a pre-catalyst for the oxidation of sulfur compounds, and possibly several other classes of complexes.

Treatment of this catalytically inactive aqueous solution of 5 with Rb^+ facilitates isolation, crystallization and characterization of a hydroxy-bridged dimer,

$Rb_{11}[\{(\beta-SiFe_2W_{10}O_{37}(OH)(H_2O))_2(\mu-OH)\}]^{11-}$, a POM in which the initial γ - Fe_2 Keggin units have rearranged to β - Fe_2 Keggin units (X-ray structure in Figure 7). This finding leads to two substantive implications for POM-based catalytic systems: (1) the proximal arrangement of d-electron centers seen in the γ - XW_{10} POM structures is important for catalysis (other isomers including the β isomer with adjacent Fe centers in the complex at right, are less catalytically active or inactive); and (2) the β isomer of the Keggin structure is more stable

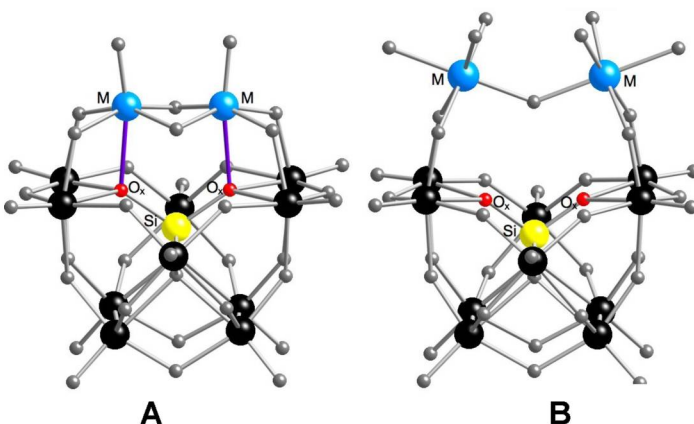


Figure 6. Two known structural forms of the polyanion with adjacent interacting d-electron centers (“M” in blue; $M = Fe^{II}$), the γ -disubstituted Keggin POM. **A:** the in-pocket form -- blue M centers are bonded to the oxygen, O_x (red) on the central heteroatom (yellow; Si in this case). **B:** The out-of-pocket form -- blue M centers not bonded to O_x .

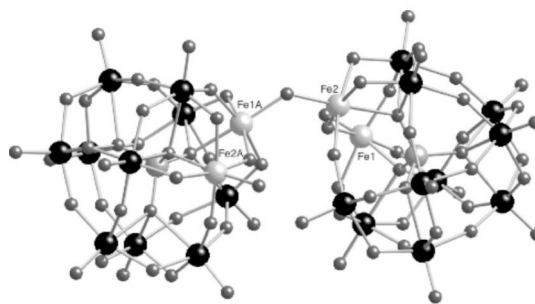


Figure 7. X-ray structure of Rb_{11} salt of $[\{(\beta-SiFe_2W_{10}O_{37}(OH)(H_2O))_2(\mu-OH)\}]^{11-}$ the POM resulting from rearrangement of the trimer, 4, in H_2O during catalysis.

thermodynamically, at least in H₂O and protic media, than the γ isomer, a finding consistent with previous experimental and computational studies.

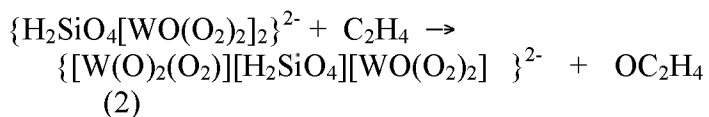
We validated the use of density functional methods to study di-d-electron metal-substituted γ -Keggin POM anions. For this purpose we evaluated the geometrical and electronic structures of $[\gamma(1,2)\text{-SiW}_{10}\{\text{Mn}(\text{OH})_2\}_2\text{O}_{38}]^{4-}$, and the divacant lacunary silicodecatungstate, $\gamma\text{-}[\text{SiW}_{10}\text{O}_{36}]^{8-}$. This approach was shown to adequately describe the geometries of these classes of species.

The validated computational approaches were employed to elucidate the electronic and geometrical structures of the di-transition metal substituted γ -Keggin POMs with the formula $[\gamma\text{-X}^{n+}(\text{M}^{\text{III}}_2(\text{OH})_2)(\text{M}_{\text{FM}})_{10}\text{O}_{36}]^{(8-n)-}$, where $\text{M}_{\text{FM}} = \text{Mo}$ and W ; $\text{X} = \text{Al}^{\text{III}}$, Si^{IV} , P^{V} and S^{VI} , and $\text{M} = \text{Mn}$, Fe , Mo , Ru and Rh . Our objectives were to elucidate roles of chemical composition (X , M and M_{FW}) of structurally and catalytically attractive polytungstates and polymolybdates on their geometries, electronic structures, and magnetic properties.

We also study structure and reactivity of the lacunary POM, $[\gamma\text{-SiW}_{10}\text{O}_{34}(\text{H}_2\text{O})_2]^{4-}$. It was found that this complex catalyzes selective epoxidation of alkenes using H₂O₂ as the oxidant. Utilizing these new data, a mechanism for H₂O₂-based epoxidation of olefins catalyzed by the lacunary polyoxometalate (POM) $[\gamma\text{-SiW}_{10}\text{O}_{36}\text{H}_4]^{4-}$ was defined for the first time. We demonstrate that a proximal counter cation significantly reduces the rate-limiting barrier and is key to making this di-lacunary silicotungstate a very efficient catalyst for the epoxidation of olefins by hydrogen peroxide.

The mechanisms of olefin epoxidation by hydrogen peroxide catalyzed by $[\gamma\text{-1,2-H}_2\text{SiV}_2\text{W}_{10}\text{O}_{40}]^{4-}$, **7** were studied using the density functional (B3LYP) approach. The roles of solvent and the counter cation are taken into account. It was shown that the formation of the vanadium-hydroperoxo species with a $\{\text{OV}-(\mu\text{-OOH})(\mu\text{-OH})\text{-VO}\}(\text{H}_2\text{O})$ core from **7** and H₂O₂ is a very facile process. From this intermediate, reaction proceeds via two distinct pathways: “hydroperoxo” and “peroxo”. We predicted that the $[\gamma\text{-1,2-H}_2\text{SiV}_2\text{W}_{10}\text{O}_{40}]^{4-}$ -catalyzed olefin epoxidation by H₂O₂ most likely occurs via a “water-assisted peroxo” pathway.

We also elucidated the mechanism of the ethylene epoxidation by $\{\text{H}_2\text{SiO}_4[\text{WO}(\text{O}_2)_2]_2\}^{2-}$ polyperoxytungstate (PPT, see Figure 8). It was shown that the reaction



is a very facile process, occurs with an energy barrier of only 12-17 kcal/mol, and is highly exothermic.

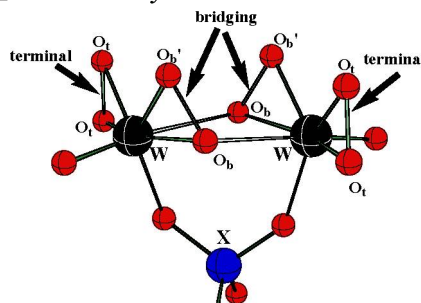
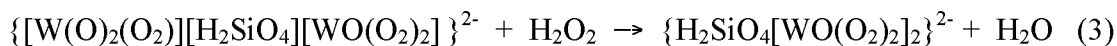


Figure 8. Schematic presentation of the polyperoxytungstate (PPT) and its possible reactive peroxo ligands

Interestingly, an O-atom transfer from the “bridging” peroxo ligand to olefin occurs with a few (2-3) kcal/mol lower barrier than that from the “terminal” peroxo ligand.

Regeneration of the catalyst by hydrogen peroxide (H₂O₂), i. e. the reaction:



is a multi-step process and occurs with a rate-determining barrier of 13-20 kcal/mol corresponding to the H-atom transfer from the coordinated hydrogen peroxide to one of the oxo ligands to form $\{[\text{WO}(\text{OH})(\text{OOH})(\text{O}_2)][\text{H}_2\text{SiO}_4][\text{WO}(\text{O}_2)_2]\}^{4-}$. In the next stage, this intermediate undergoes several transformations and produces the final products $\{\text{H}_2\text{SiO}_4[\text{WO}(\text{O}_2)_2]\}^{2-} + \text{H}_2\text{O}$ via H-atom transfer from OOH group to OH with a barrier of only 4-6 kcal/mol. This process is found to be almost thermoneutral.

We investigated the role of the heteroatom ($X = \text{Si}^{\text{IV}}$, P^{V} , and S^{VI}) on the reactivity of $\{\gamma\text{-}[(\text{H}_2\text{O})\text{Ru}^{\text{III}}(\mu\text{-OH})_2\text{Ru}^{\text{III}}(\text{H}_2\text{O})][\text{X}^{\text{n+}}\text{W}_{10}\text{O}_{36}]\}^{(8-\text{n})-}$ with the O₂ molecule. It was shown that the nature of X only slightly affects the reactivity of these complexes with O₂. The overall reaction (2) proceeds with moderate energy barriers for all studied X's and is exothermic.

III. Computational method development.

Complementing the efforts presented above was the development of less time-consuming but reasonably accurate computational methods allowing one to explore more deeply large catalytic systems.

Parameters have been developed for five first-row transition metal elements (Sc, Ti, Fe, Co and Ni) in combination with H, C, N, O, as well as the same metal (M-M) for the spin-polarized self-consistent-charge density-functional tight-binding (DFTB) method. Test results show that the DFTB method with the present parameters in most cases reproduces structural properties very well, but the bond energies and the relative energies of different spin states only qualitatively compare to the most accurate results. These parameters are made available as part of the DFTB code.

We also developed “reactive” force fields (ReaxFF) parameters for several Lindqvist POM's (see Figure 9).

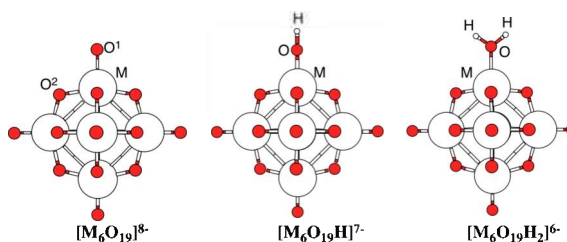
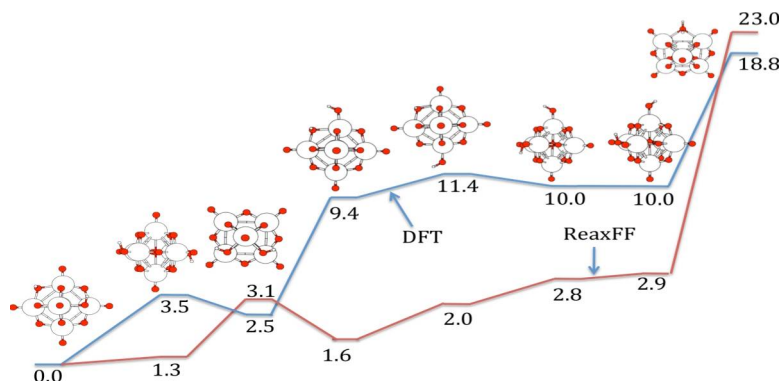


Figure 9. Three “canonical” structures of $[\text{M}_6\text{O}_{19}\text{H}_x]^{(8-x)-}$, where $x = 0, 1, 2$; and $M = \text{Nb}, \text{Ta}$

In order to validate of our ReaxFF parameters, we calculated structures of $[\text{H}_x\text{M}_6\text{O}_{19}]^{(8-x)-}$ (where $x = 0, 1$ and 2 , and $M = \text{Nb}$ and Ta) as well as their numerous isomers of $[\text{M}_6\text{O}_{19}(\text{H}_2\text{O})]^{8-}$ at the ReaxFF and B3LYP/ $\{\text{LanL2DZ} + [6\text{-}31\text{+G}(\text{d,p})_{\text{O,H}}]\}$ level of theory. Comparison of these data clearly shows that the overall structure, bonding character, i.e., single vs. double bond difference, as well as thermodynamic properties of these Lindqvist ions are reproduced reasonably well by ReaxFF. These parameters are made available as part of the ReaxFF code.

After establishing that ReaxFF is capable of describing the basic features of $[\text{H}_x\text{M}_6\text{O}_{19}]^{(8-x)}$ (where $x = 0, 1$ and 2 , and $\text{M} = \text{Nb}$ and Ta), our next step was modeling of solvation dynamics of these POMs. Molecular dynamics simulations (MD) run at $\sim 150\text{K}$ for 10 ps , following an initial geometry relaxation, show small fluctuations of a rigid metal cage, which is characteristic of low temperature dynamics.

Figure 10. Schematic presentation of relative energies (in kcal/mol) of numerous isomers of the $[\text{Nb}_6\text{O}_{19}(\text{H})_2]^{6-}$ ion.



Publications:

a. Sole funding by DOE-BES:

1. Anderson, T. M.; Fang, X.; Mbomekalle, I. M.; Keita, B.; Nadjo, L.; Hardcastle, K. I.; Farsidjani, A.; Hill, C. L. "Structural and Electrochemical Studies of Dicupric Sandwich-Type Complexes" *J. Cluster Sci.* **2006**, *17*, 183-196. (Invited ms for M. T. Pope special issue).
2. Musaev, D. G.; Geletti, Y. V.; Hill, C. L.; Morokuma, K. "Computational Modeling of Di-Transition-Metal-Substituted γ -Keggin Polyoxometalate Anions. Structural Refinement of the Protonated Divacant Lacunary", *Inorg. Chem.* **2004**, *43*, 7702-7708.
3. Anderson, T. M.; Neiwert, W. A.; Kirk, M. L.; Piccoli, P. M. B.; Schultz, A. J.; Koetzle, T. F.; Musaev, D. G.; Morokuma, K.; Cao, R.; Hill, C. L. "A late-transition metal oxo complex: $\text{K}_7\text{Na}_9[\text{O}=\text{Pt}^{\text{IV}}(\text{H}_2\text{O})\text{L}_2]$, $\text{L} = [\text{PW}_9\text{O}_{34}]^{9-}$ ", *Science*, **2004**, *306*, 2074-2077.
4. Botar, B.; Geletti, Y. V.; Kögerler, P.; Musaev, D. G.; Morokuma, K.; Weinstock, I. A.; Hill, C. L. "Asymmetric terminal ligation on substituted sites in a disorder-free Keggin anion, $[\text{b-SiFe}_2\text{W}_{10}\text{O}_{36}(\text{OH})_2(\text{H}_2\text{O})\text{Cl}]^{5-}$ ", *Dalton Trans.* **2005**, 2017-2021.
5. Anderson, T. M.; Cao, R.; Slonkina, E.; Hedman, B.; Hodgson, K. O.; Hardcastle, K. I.; Neiwert, W. A.; Wu, S.-X.; Kirk, M. L.; Knottenbelt, S.; Depperman, E. C.; Musaev, D. G.; Morokuma, K.; Hill, C. L. "A Palladium-Oxo Complex. Stabilization of this Proposed Catalytic Intermediate by an Encapsulating Polytungstate Ligand" *J. Am. Chem. Soc.* **2005** *127*, 11948-11949.
6. Wang, Y.; Zheng, G.; Morokuma, K.; Geletii, Y. V.; Hill, C. L.; Musaev, D. G., "Density Functional Study of the Roles of Chemical Composition of Di-Transition-

- Metal-Substituted *g*-Keggin Polyoxometalate Anions”, *J. Phys. Chem. B*, **2006**, *110*, 5230-5237.
7. Quinonero, D.; Morokuma, K.; Khavrutskii, L. A.; Botar, B.; Geletii, Y. V.; Hill, C. L.; Musaev, D. G., “The role of the central atom in structure and reactivity of polyoxometalates with adjacent d-electron metal sites. Computational and experimental study of γ - $[(X^{n+}O_4)Ru_2(OH)_2W_{10}O_{32}]^{(8-n)-}$, X = Al^{III}, Si^{IV}, P^V and S^{VI}.” *J. Phys. Chem. B*, **2006**, *110*, 170-173.
 8. Prabhakar, R.; Morokuma, K.; Hill, C. L.; Musaev, D. G. “Insights into the Mechanism of Selective Olefin Epoxidation Catalyzed by $[\gamma-(SiO_4)W_{10}O_{32}H_4]^{4+}$. A Computational Study” *Inorg. Chem.* **2006**, *45*, 5703-5709.
 9. Botar, B.; Kögerler, P.; Hill, C. L. “A nanoring-nanosphere molecule, $\{Mo_{214}V_{30}\}$. Pushing the boundaries of controllable inorganic structural organization at the molecular level”, *J. Am. Chem. Soc.* **2006**, *128*, 5336-5337.
 10. Quiñonero, D.; Morokuma, K.; Geletii, Y. V.; Hill, C. L.; Musaev, D. G. “A Density Functional Study of Geometry and Electronic Structure of $[(SiO_4)(M^{III})_2(OH)_2W_{10}O_{32}]^{4+}$ for M = Mo, Ru and Rh.” *J. Mol. Catal. A, Chem.* **2007**, *262*, 227-235.
 11. Fang, X.; Hill, C. L. “Multiple Reversible Protonation of Polyoxoanion Surfaces: Direct Observation of Dynamic Structural Effects from Proton Transfer”, *Angew. Chem. Int. Ed.* **2007**, *46*, 3877–3888
 12. Botar, B.; Kögerler, P.; Hill, C. L. “Tetrairon and Hexairon Hydroxo/Acetato Clusters Stabilized by Multiple Polyoxometalate Scaffolds. Structures, Magnetic Properties and Chemistry of a Dimer and a Trimer”, *Inorg. Chem.* **2007**, *46*, 5398-5403.
 13. Prabhakar, R.; Morokuma, K.; Geletii, Y. V.; Hill, C. L.; Musaev, D. G. “Insights into the Mechanism of H₂O₂-based Olefin Epoxidation Catalyzed by the Lacunary $[\gamma-(SiO_4)W_{10}O_{32}H_4]^{4+}$ and di-V-substituted- γ -Keggin $[\gamma-1,2-H_2SiV_2W_{10}O_{40}]^{4+}$ Polyoxometalates. A Computational Study.” In "Computational Modeling for Homogenous and Enzymatic Catalysis", Morokuma, K.; Musaev, D. G. Eds. Wiley: New York, **2008**, 215-230.
 14. Kuznetsov, A. E.; Geletii, Y. V.; Hill, C. L.; Morokuma, K.; Musaev, D. G. “On the Mechanism of the Divanadium-substituted Polyoxotungstate $[\gamma-1,2-H_2SiV_2W_{10}O_{40}]^{4+}$ Catalyzed Olefin Epoxidation by H₂O₂: A Computational Study.” *Inorg. Chem.*, **2009**, *48*, 1871-1878.
 15. Kuznetsov, A. E.; Geletii, Y. V.; Hill, C. L.; Morokuma, K.; Musaev, D. G. “Dioxygen and Water Activation Processes on Multi-Ru-substituted Polyoxometalates: Comparison with the “Blue Dimer” Water Oxidation Catalyst” *J. Am. Chem. Soc.* **2009**, *131*, 6844-6854.
 16. Y. V. Geletii, C. Besson, Y. Hou, Q. Yin, D. G. Musaev, D. Quinonero, R. Cao, K. I. Hardcastle, A. Proust, P. Kögerler, C. L. Hill, “Structural, Physicochemical and Reactivity Properties of and All-Inorganic Catalyst for Water Oxidation”, *J. Am. Chem. Soc.* **2009**, *131*, 17360-17370.
 17. Claire Besson, Djameladdin G. Musaev, Vanina Lahootun, Rui Cao, Lise-Marie Chamoreau, Richard Villanneau, Françoise Villain, René Thouvenot, Yurii V. Geletii, Craig L. Hill, Anna Proust, “Vicinal di-nitridoruthenium substituted polyoxometalates, γ - $[XW_{10}O_{38}\{RuN\}_2]^{6-}$ (X=Si or Ge)”, *Eur. J. Chem.* **2009**, *15*, 10233-10243.

18. Besson, C.; Geletii, Y. V.; Villain, F.; Villanneau, R.; Hill, C. L.; Proust, A. "Nitrogen-atom transfer from $[\text{PW}_{11}\text{O}_{39}\text{Ru}^{\text{VI}}\text{N}]^{4-}$ to PPh_3 ", *Inorg. Chem.* **2009**, 48(19), 9436-9443.
19. Kuznetsov, A. E.; Geletii, Y. V.; Hill, C. L.; Musaev, D. G. "Insights into mechanism of O_2 formation and release from the $\text{Mn}_4\text{O}_4\text{L}_6$ 'cubane' cluster", *J. Phys. Chem. A*, **2010**, 114, pp 11417-11424.
20. Quinonero, D.; Kaledin, A.; Kuznetsov, A. E.; Geletii, Y. V.; Besson, C.; Hill, C. L.; Musaev, D. G. "Computational studies of the geometry and electronic structure of an all-inorganic and homogeneous tetra-Ru-polyoxometalate catalyst for water oxidation and its four subsequent one-electron oxidized forms", *J. Phys. Chem. A*, **2010**, 114 (1), pp 535-542
21. Yin, Q.; Tan, J. M.; Besson, C.; Geletii, Y. V.; Musaev, D. G.; Kuznetsov, A. E.; Luo, Z.; Hardcastle, K. I.; Hill, C. L. "A soluble molecular fast organic-structure-free water oxidation catalyst based on abundant metals", *Science*, **2010**, 328, 342-345.
22. Kuznetsov, A. E.; Geletii, Y. V.; Hill, C. L.; Morokuma, K.; Musaev, D. G. "The Effect of the Heteroatom on the Reactivity of Di-Ru-substituted Polyoxometalates $\{\gamma\text{-}[\text{Ru}^{\text{III}}(\mu\text{-OH})_2\text{Ru}^{\text{III}}][(\text{X}^{\text{n+}}\text{O}_4)\text{W}_{10}\text{O}_{32}]\}^{(8-\text{n})-}$ Towards Dioxygen and Water Activation: Comparison of $\text{X} = \text{P}^{\text{V}}$ and S^{VI} with Si^{IV} ", *Theo. Chem Acc.*, **2011**, 130, 197-207.
23. Geletii, Y. V.; Yin, Q.; Hou, Y.; Huang, Z.; Ma, H.; Song, J.; Besson, C.; Luo, Z.; Cao, R.; Halloran, K. P. O.; Zhu, G.; Zhao, C.; Vickers, J. W.; Ding, Y.; Mohebbi, S.; Kuznetsov, A. E.; Musaev, D. G.; Lian, T.; Hill, C. L. "Polyoxometalates in the design of effective and tunable water oxidation catalysts", *Isr. J. Chem.*, **2011**, 51, pp 238-246.
24. Zhu, G.; Geletii, Y. V.; Kögerler, P.; Schilder, H.; Song, J.; Lense, S.; Zhao, C.; Hardcastle, K. I.; Musaev, D. G.; Hill, C. L.; "Water oxidation catalyzed by a new tetracobalt-substituted polyoxometalate complex: $\{[\text{Co}_4(\mu\text{-OH})(\text{H}_2\text{O})_3](\text{Si}_2\text{W}_{19}\text{O}_{70})\}^{11-}$ ", *Dalton Trans.*, **2012**, 41, 2084-2090.
25. Kaledin, A. L.; van Duin, A.C.T.; Hill, C. L.; Musaev, D. G. "Parameterization of Reactive Force Field: Dynamics of the $[\text{H}_x\text{Nb}_6\text{O}_{19}]^{(8-x)}$ Lindqvist Polyoxoanion in Bulk Water", *J. Phys. Chem. A*, **2013**, 117, 6967-6974

b. Joint funding by DOE and other Sources:

26. Botar, B.; Geletii, Y. V.; Kögeler, P.; Musaev, D. G.; Morokuma, K.; Weinstock, I. A.; Hill, C. L. "The True Nature of the Diiron(III) γ -Keggin Structure in Water. Catalytic Aerobic Oxidation and Chemistry of an Unsymmetrical Trimer" *J. Am. Chem. Soc.* **2006**, 128, 11268-11277.
27. Geletii, Y. V.; Hill, C. L.; Atalla, R. H.; Weinstock, I. A. "Reduction of O_2 to Superoxide Anion ($\text{O}_2^{\bullet-}$) in Water by Heteropolytungstate Cluster-Anions" *J. Am. Chem. Soc.* **2006**, 128, 17033-17042.
28. Hill, C. L.; Anderson, T. M.; Han, J.-W.; Hillesheim, D. A.; Geletii, Y. V.; Okun, N. M.; Cao, R.; Botar, B.; Musaev, D. G.; Morokuma, K. "New complexes and materials for O_2 -based oxidations.", *J. Mol. Catal. A, Chem.* **2006**, 251, 234-238.
29. Zheng, G.; Witek, H.; Bobadova-Parvanova, P.; Irle, S.; Musaev, D. G.; Prabhakar, R.; Morokuma, K.; Lundberg, M.; Elstner, M.; Kohler, C.; Frauenheim, T.

- “Parameterization of Transition Metal Elements for the Spin-Polarized Self-Consistent-Charge Density-Functional Tight-Binding Method: 1. Parameterization of Ti, Fe, Co, and Ni.” *J. Chem. Theory and Comp.*, **2007**, 3(4); 1349-1367.
30. Cao, R.; Anderson, T. M.; Piccoli, P. M. B.; Schultz, A. J.; Koetzle, T. F. Geletii, Y. V.; Slonkina, E.; Hedman, B.; Hodgson, K. O.; Hardcastle, K. I.; Fang, X.; Kirk, M. L.; Knottenbelt, S.; Kögerler, P.; Musaev, D. G.; Morokuma, K.; Hill, C. L. “Reactive terminal gold-oxo units” *J. Am. Chem. Soc.*, **2007**, 129(36); 11118-11133.
31. Hill, C. L. “Terminal oxo complexes of the catalytically important noble metals realized.” *Chem. in Australia*, **2007**, 74, 17-18.
32. Hill, C. L.; Delannoy, L.; Duncan, D. C.; Weinstock, I. A.; Renneke, R. F.; Reiner, R. S.; Atalla, R. H.; Han, J. W.; Hillesheim, D. A.; Cao, R.; Anderson, T.; Okun, N. M.; Musaev, D. G.; Geletii, Y. “Complex catalysts from self repairing ensembles to highly reactive air-based oxidation systems” *Comptes Rendus Chimie*, **2007**, 10, 305-312.
33. Hill, C. L. “Progress and challenges in polyoxometalate-based catalysis and catalytic materials chemistry”, *J. Mol. Catal. A., Chem.* **2007**, 262, 2-6.
34. Yurii V. Geletii, Bogdan Botar, Paul Kogerler, Daniel A. Hillesheim, Djameladdin G. Musaev, Craig L. Hill, „An All-Inorganic, Stable, and Highly Active Tetraruthenium Homogenous Catalyst for Water Oxidation“, *Angew. Chem. Intern. Ed.* **2008**, 47, 3896-3899. *Selected as the VIP (“Very Important Article”) by the reviewers and editor.*
35. Rui Cao, Jong Woo Han, Traves M. Anderson, Daniel A. Hillesheim, Martin L. Kirk, Djameladdin G. Musaev, Keijji Morokuma, Yurii V. Geletii, Craig L. Hill, „Late Transition Metal Oxo Compounds and Open Framework Materials that Catalyze Aerobic Oxidations“, *Prog. Inorg. Chem.*, **2008**, pp.245-272.